Invited talk at the SLAC Summer Institute
on Particle Physics, 11-22 July 1977,
Stanford, California

LBL-6766

ANOMALOUS ELECTRON PRODUCTION IN THE LEAD-GLASS WALL EXPERIMENT AT SPEAR*

Ronald J. Madaras

October 1977

NOTICE
This report was prepared as an account of work sponsored by the United States Government. Neither the United States nor the United States Department of Energy, nor any of their employees, nor any of their contractors, subcontractors, or their employees, makes any warranty, express or implied, or assumes any legal liability or responsibility for the accuracy, completeness or usefulness of any information, apparatus, product or process disclosed, or represents that its use would not infringe privately owned rights.

*Work supported by the Energy Research and Development Administration.

DISTRIBUTION OF THIS DOCUMENT IS UNLIMITED

ANOMALOUS ELECTRON PRODUCTION IN THE LEAD-GLASS WALL EXPERIMENT AT SPEAR

Ronald J. Madaras
Lawrence Berkeley Laboratory
University of California
Berkeley, California 94720

I. INTRODUCTION

In this talk I will present the latest results of the Lead-Glass Wall Collaboration[1] on anomalous electron production[2] in electron-positron annihilations at SPEAR at center-of-mass energies from 3.77 to 7.4 GeV. This experiment, having SLAC number SP-26, ran at SPEAR from October 1976 through June 1977. The data were collected with the SLAC-LBL Mark I magnetic detector,[3] which was modified by the addition of a lead-glass detector for improved electron and photon identification.

Anomalous electrons in electron-positron annihilations can come from at least two possible sources:

1. Heavy lepton production and decay: For example,

$$e^+e^- \to \tau^+ + \tau^- \qquad (1)$$
$$\tau^+ \to e^+\nu_e\bar{\nu}_\tau \qquad \tau^- \to \mu^-\bar{\nu}_\mu\nu_\tau,\ \pi^-\nu_\tau,\ \rho^-\nu_\tau,\ \vdots$$

Evidence for the heavy lepton, τ, was first found by M. L. Perl[4,5] in 1975, and has been confirmed by further experiments at SPEAR[6-9] and at DORIS.[10-13] The predicted branching ratios for various decay modes of the heavy lepton can be found in Table I.[14] It is seen that the heavy lepton decays into a single charged particle about 85% of the time, so that most of the events of type (1) above will have only two charged particles in the final state.

Table I. Predicted branching ratios for a τ^- charged lepton of mass 1.9 GeV/c^2, an associated neutrino mass of 0.0, and V-A weak interaction coupling.[14]

Decay mode	Branching ratio	Number of charged particles in final state
$e^- \bar{\nu}_e \nu_\tau$	0.20	1
$\mu^- \bar{\nu}_\mu \nu_\tau$	0.20	1
$\pi^- \nu_\tau$	0.11	1
$K^- \nu_\tau$	0.01	1
$\rho^- \nu_\tau$	0.22	1
$K^{*-} \nu_\tau$	0.01	1
$A_1^- \nu_\tau$	0.07	1, 3
(hadron continuum)$^- \nu_\tau$	0.18	1, 3, 5

2. Charmed particle production and decay: For example,

$$e^+e^- \to D + \bar{D} + n \cdot \text{hadrons} \quad (n \geq 0) \qquad (2)$$

$$D \to eK\nu,\ eK^*\nu,\ \vdots \qquad \bar{D} \to K\pi,\ K\pi\pi,\ \vdots$$

It is expected that most of the events of this type will have four or more charged particles in the final state. For example, at the $\psi(3772)$[15] where $D\bar{D}$ with no other hadrons is produced, about 90% of the events of type (2) will contain four or more charged particles. At higher center-of-mass energies, where D^*D^* or $D^*D^*\pi\pi$ are produced, the percentage is higher. Of course, even when four particles are produced, fewer might be detected because the detector doesn't cover the full 4π sr solid angle.

Thus in our analysis, we have divided up the anomalous electron events into two classes:

Two-prong events of the type $e^+ + e^- \to e^\pm + \mu^\mp + n \cdot \gamma$ or $e^\pm + h^\mp + n \cdot \gamma$, with $n \geq 0$ ($h \equiv$ hadron). Two, and only two, charged particles are detected.

Multiprong events of the type $e^+ + e^- \to e^\pm + (\geq 2$ charged particles$) + n \cdot \gamma$, with $n \geq 0$. Here at least three charged particles are detected.

We analyze these two classes of events separately in order to separate the charm and heavy lepton signals, as we have seen above that heavy lepton events of type (1) will mainly be two-prong events and that charm events of type (2) will mainly be multiprong events.

In Section II of this talk I will describe the lead-glass detector, and in Section III I will discuss the details of the identification of electrons using this detector. In Section IV I will discuss the results of the analysis of the two-prong events, and give our values for the branching ratios $B(\tau \to e\, \nu_e \nu_\tau)$ and $B(\tau \to h + \text{neutrals})$. In Section V I will discuss the results of the analysis of the multiprong events, and give both the semi-leptonic branching ratio of the charmed D meson into electrons and the semi-leptonic branching ratio of "charmed particles" into electrons for various electron-positron center-of-mass energies.

II. LEAD-GLASS WALL DETECTOR

In order to improve the identification of electrons, we have replaced one octant of the magnet return yoke of the SLAC-LBL Mark I magnetic detector with two layers of lead-glass counters interspersed with magnetostrictive spark chambers. These are shown schematically in Figure 1, and in more detail in Figure 2. The shower counters which were in that octant have been replaced by 1.9 cm-thick scintillation counters. The lead-glass system consists of:

1. a 2 x 26 array of lead-glass "active converters" (AC), 3.3 X_0 deep, having dimensions 10 x 11 x 90 cm, followed by:

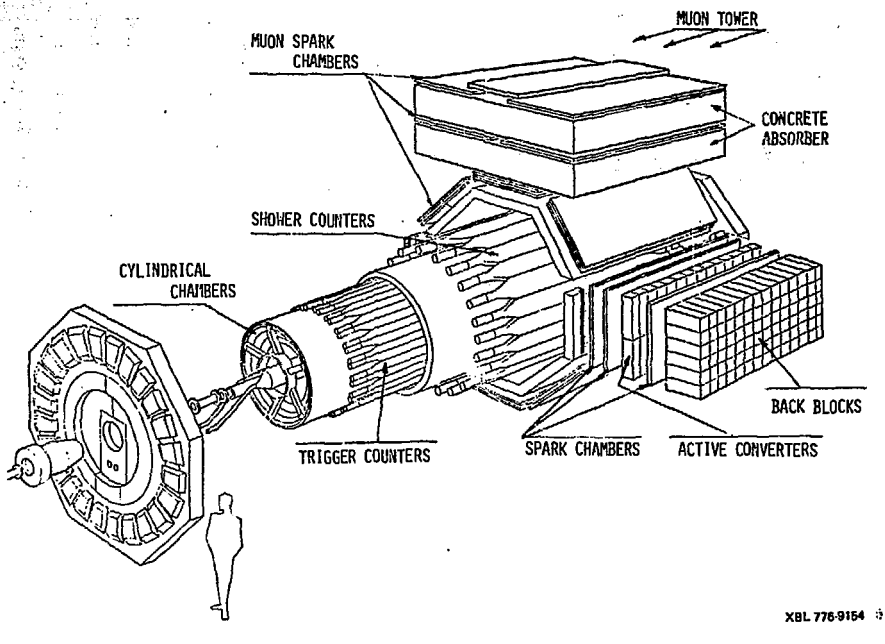

Fig. 1 Exploded view of the SLAC-LBL Mark I magnetic detector with the addition of the Lead-Glass Wall Detector.

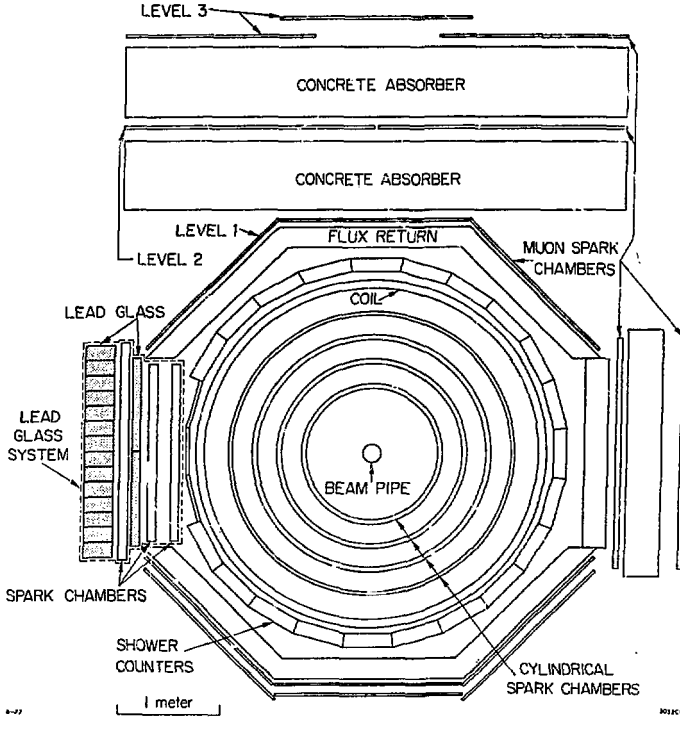

Fig. 2 The SLAC-LBL Mark I magnetic detector with the addition of the Lead-Glass Wall Detector, in a view along the beam line. The two proportional chambers around the beam pipe and the trigger counters are not shown.

2. a 14 x 19 array of lead-glass "back-block counters" (BB), 10.5 X_o deep, having dimensions 15 x 15 x 32 cm, and

3. a set of three magnetostrictive spark chambers.

Each active converter (back block) lead-glass counter was viewed through a lucite lightguide by an EMI 3.5" 9531 R (5" 9618 R) photomultiplier tube. The anode signal from each counter was sent to an ADC in a LBL Large-Scale Digitizer System,[16] and the dynode signals of the counters were summed in rows and used for triggering. Both lead-glass arrays were kept in closed boxes where temperatures were kept constant. The lead-glass system covered polar angles $60° < \theta < 120°$ and azimuthal angles $-20° < \phi < 20°$, and thus covered ~ 6% of 4π sr solid angle.[17]

The lead-glass counters were initially calibrated to an accuracy of ~ 10% by using several radioactive sources. These sources were small thallium doped NaI scintillation crystals diffused with Americium-241, and they themselves were calibrated with several lead-glass counters in an electron beam at SLAC. The final calibration of the gains of all the lead-glass counters was done using electrons of known energy from Bhabha scattering events obtained during the data taking at SPEAR. With this method, the calibration constants of the counters are obtained by minimizing the square of the energy resolution of the counters for the Bhabha events, with the constraint that the average energy deposited in the lead-glass is equal to the actual energy of the Bhabhas. This final calibration has an accuracy of about 5%. The response of the lead-glass system (LGW) to a set of high-energy Bhabha electrons (which were <u>not</u> used in the above calibration) is shown in Figure 3. The energy resolution of the <u>whole</u> system is given by $\sigma/E = 9\%/\sqrt{E}$ (E in GeV). This resolution is degraded from the intrinsic resolution of the counters of $5\%/\sqrt{E}$ due to the presence of the 1 X_o aluminum coil of the Mark I magnet which is before the lead-glass system (see Figure 2).

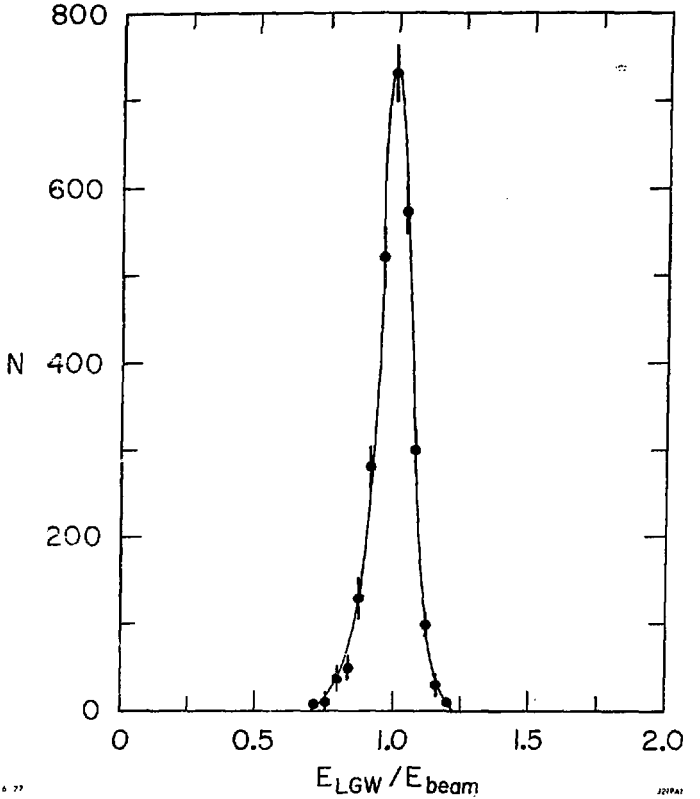

Fig. 3 Distribution of the total energy, E_{LGW}, measured in the whole lead-glass wall (back blocks and active converters) for electrons from Bhabha scattering ($e^+e^- \rightarrow e^+e^-$). E_{BEAM} is 3.2-3.7 GeV. The energy resolution is $\sigma_{E_{LGW}}/E_{LGW} = 5.1\%$.

In order to keep the energy resolution of the whole system of lead-glass counters constant over the ten-month life of the experiment, one has to accurately monitor the gains of each of the 318 counters during this time. This has been successfully achieved with an LED monitoring system[18] which has tracked the gains of the lead-glass counters throughout the experiment with a precision of 1-2%. This system is shown schematically in Figure 4. The light source is a single high-intensity yellow LED, and the light is transmitted to each of the counters via low-attenuation plastic optical fibers. The LED light is monitored using a reference scintillation counter, whose gain is known from frequent ^{241}Am-NaI source and cosmic ray measurements.

III. ELECTRON IDENTIFICATION USING THE LEAD GLASS WALL DETECTOR

A. Cuts. The identification of a particle that enters the Lead-Glass Wall (LGW) is based on its time-of-flight and on the energy deposited in each of the two layers of lead-glass counters. To identify a particle as an electron candidate we require:

1. The particle's momentum, as measured in the Mark I detector, is greater than 300 MeV/c for multiprong events and 400 MeV/c for two-prong events.

2. The measured time-of-flight of the particle agrees with that expected for an electron within two standard deviations (0.8 ns). This reduces the background from misidentification of kaons and protons.

3. The particle is within the fiducial volume of lead-glass.

4. No other charged or neutral particles in the LGW are nearby.

5. The energy deposited in the lead-glass back blocks (E_{BB}) is greater than 10% of the momentum of the particle. (This requirement only exists for the multiprong events.)

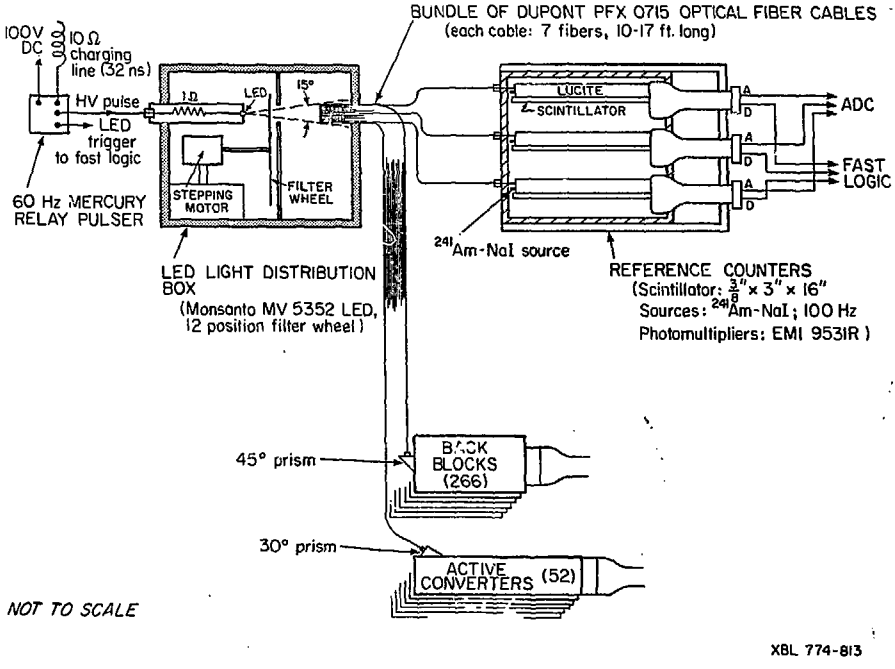

Fig. 4 A schematic diagram of the LED monitoring system for the lead-glass counters.

6. The energy deposited in the lead-glass active converters (E_{AC}) is substantially greater than the 80 MeV expected for a noninteracting particle:

2-prong events: $E_{AC} > 150$ MeV

multiprong events: $E_{AC} > \text{Max}\ (150,\ 250 \cdot p)$
where p is the particle momentum in GeV/c

7. The total energy deposited in the LGW ($E_{LGW} = E_{AC} + E_{BB}$) is approximately equal to the momentum of the particle:

2-prong events: $1.50 > E_{LGW}/p > 0.65$

multiprong events: $1.50 > E_{LGW}/p > \text{Min}[0.80,\ 0.65+0.15 \cdot (p-0.4)]$
(p in Gev/c)

The requirements on the energies deposited in the lead-glass are more severe for the multiprong events than for the two-prong events, because the hadron background is a much larger fraction of the anomalous electron signal for the multiprong events than for the two-prong events.

B. Detection Efficiency. The LGW electron identification efficiency (ε) for the above cuts on the energy deposited in the lead-glass counters is measured using electrons from the reactions $e^+e^- \to e^+e^-\gamma$ and $e^+e^-e^+e^-$. These events are found by requiring two (and only two) oppositely charged coplanar particles which have most of the missing momentum going along the beam direction. In addition, we require that there are no photons detected and that the particle outside the LGW is determined to be an electron by the Mark I detector. The detection efficiency for the electron in the LGW is measured to be:

2-prong event LGW cuts: $\varepsilon = 75\%$ ($p_e = 400$ MeV/c) to 98% ($p_e > 1.0$ GeV/c), with $\bar{\varepsilon} = 89\%$.

multiprong event LGW cuts: $\varepsilon = 55\%$ ($p_e = 300$ MeV/c) to 90% ($p_e > 1.0$ GeV/c). with $\bar{\varepsilon} \sim 75\%$

The detection efficiency is smaller for the LGW energy cuts appropriate for the multiprong events than for the two-prong events, becuase the cuts are more severe for the multiprong events (see Section III A.).

C. Backgrounds. Important backgrounds to the anomalous electron signal are:

(a) misidentification of hadrons which interact in the magnet coil or active converters so as to satisfy the above requirements on the energy deposited in the lead-glass,

(b) pion and kaon decay,

(c) photon conversions in the beampipe, pipe counters or MWPC (total of 0.052 X_0), or Dalitz decays of π^0's and η's, where both the electron and positron are detected by the Mark I detector.

(d) asymmetric electron-positron pairs from photon conversions or Dalitz decays where one member of the pair is unobserved because its momentum is below the threshold for efficient detection in Mark I (~ 100 MeV/c).

The background due to (c) is eliminated by rejecting electron candidates that have a small opening angle with a particle of opposite electric charge.

We determine the background due to (a), (b) and (d) at various center-of-mass energies in three steps:

i) First, at a center-of-mass energy where we think there is no anomalous electron production, we measure the fraction of particles in the LGW that pass all our cuts defining an electron. This we assume is our basic background rate from (a), (b) and (d). We choose to do this at the $\psi(3095)$, as it is below threshold for charm and heavy lepton production. Using multihadronic events there, we find that 1.4% of all the particles in the LGW which have a momentum of 300 MeV/c are identified as electrons. This fraction decreases with momentum to 0.4% per particle at 1.0 GeV/c.

ii) Second, we assume that the background per particle in the LGW due to (a) and (b) does not change as we go from the $\psi(3095)$ to the highest

center-of-mass energy of 7.4 GeV. This assumption is not crucial for (b), as the background due to this source is estimated to be < 0.05% per particle.

iii) Third, we determine the additional background rate from asymmetric photon conversions or Dalitz decays (i.e. source (d)) that we might have when we go to higher center-of-mass energies. This background rate can increase with the center-of-mass energy due to increases in the number and energy of the photons and π^0's which are responsible for the background. This additional background rate was determined by measuring at several center-of-mass energies the converted e^+e^- pairs where both particles are detected, and then extrapolating with a Monte Carlo program to the case where only one particle is detected. The results are below:

Momentum (GeV/c)	Background rate due to (a), (b) and (d) as measured at $\psi(3095)$. (% per particle in LGW)	Additional background rate due to (d). (% per particle in LGW) 3.772 (GeV)	4.15 (GeV)	4.4-5.7 (GeV)	6.4-7.4 (GeV)
0.3	1.4%	0.1	0.1	0.2	0.4
0.5	1.0	0.1	0.1	0.1	0.3
0.7	0.7	0.05	0.1	0.1	0.1
≥1.0	0.4	0	0	0	0.05

As is seen, this additional background rate ranges from 0 to 0.4% per particle, with the maximum occuring for p = 0.3 GeV/c, $E_{c.m.}$ = 7.4 GeV. The increase is largest for the lowest momenta.

The average value of the total background rate due to (a), (b) and (d) is 1.1% per particle. This value is averaged over the background momentum spectrum, and is essentially the same for the four center-of-mass energy regions because the hardening of the momentum spectrum in each region compensates for the increase of the background rate in each region.

All of the above values for the background rates were obtained using the lead-glass wall energy cuts appropriate for the multiprong events (see Section III. A.). Using the looser LGW cuts appropriate for the two-prong events, one finds that the background is at most 2.0% per particle, for all momenta and center-of-mass energies.

IV. TWO-PRONG EVENTS

A. Event Sample. We recall from Section I that the "two-prong" events are of the type:

$$e^+ + e^- \to e^\pm + \mu^\mp + n \cdot \gamma$$
$$\text{or } e^\pm + h^\mp + n \cdot \gamma$$

with $n \geq 0$

h = a hadron

Two, and only two, oppositely charged particles are detected. One of them, the electron, is always identified in the lead-glass wall. The other particle is identified most of the time in the Mark I magnetic detector on the basis of information from lead-scintillator shower counters and magnetostrictive spark chambers following the 20-cm-thick iron flux return of the magnet.[19] The detection efficiencies, ε, and misidentification probabilities $P_{i \to j}$ (i.e. the probability that a particle of type i is identified as type j) for the particles identified in the Mark I detector are measured with eeγ events, $\mu\mu\gamma$ events and hadronic events with ≥ 5 charged particles. They are:

$$P_{e \to h} = 0.095 \pm 0.020 \qquad \varepsilon_e = 0.89 \pm 0.02$$
$$P_{e \to \mu} = 0.01 \pm 0.01 \qquad \varepsilon_h = 0.58 \pm 0.05$$
$$P_{\mu \to h} = 0.03 \pm 0.01 \qquad \varepsilon_\mu = 0.94 \pm 0.02$$
$$P_{h \to \mu} = 0.18 \pm 0.01$$

I will present here the results of the two-prong event analysis for data taken in three different center-of-mass energy ranges:[20]

$E_{c.m.}$ range (GeV)	Amerage $E_{c.m.}$ (GeV)	$\int$ Ldt (Pb^{-1})
4.1-4.2	4.15	1.0
4.4-5.7	4.9	2.7
6.4-7.4	6.9	5.5

The two-prong event analysis has not yet been completed for the data taken at the $\psi(3772)$.

The two-prong events are selected using the following data cuts:

1) The momentum of the particle in the lead-glass wall is > 400 MeV/c.

2) The particle in the lead-glass wall is identified as an electron using the criteria discussed in Section III.A. for two-prong events.

3) The other particle is oppositely charged, and its momentum is > 650 MeV/c to insure good identification in the Mark I detector.

4) The two charged particles are acoplanar about the incident beams by at least 20°.

5) The square of the missing mass recoiling against the two charged particles is > 0.8, 1.1 or 1.5 GeV^2, for the center-of-mass energy ranges 4.1-4.2, 4.4-5.7, and 6.4-7.4 GeV.

The last two criteria are used to reduce the background from the QED reactions: $e^+e^- \rightarrow e^+e^-$, $e^+e^-\gamma$ and $e^+e^-e^+e^-$.

For the combined data from all three center-of-mass energy regions, the number of two-prong events which pass the above cuts is listed in Table II.[6]

Table II. Two-prong events, for the combined data from $E_{c.m.}$ = 4.1-4.2, 4.4-5.7, and 6.4-7.4 GeV. See the above text for the event selection criteria. The first particle listed is always detected in the LGW (here a hadron, h, in the LGW is any particle not identified as an electron). N_γ is the detected number of γ rays associated with the events.

	Observed events		Background		Corrected events	
	$N_\gamma = 0$	$N_\gamma > 0$	$N_\gamma = 0$	$N_\gamma > 0$	$N_\gamma = 0$	$N_\gamma > 0$
eμ	21	8	0.4	1.4	21.6±6.4	3.7±4.5
eh	12	19	3.0	9.1	20.5±9.6	24.2±12.9
ee	23	71			32.1±6.9	100±14
hh	38	122			66±13	213±30

In Table II, the anomalous electron events are in the categories eμ and eh, with or without photons. The background for these events due to misidentification of ee and hh events is listed in columns 3 and 4. The last two columns list the number of anomalous electron events after corrections for the background, the misidentifications among the anomalous events themselves, and the particle detection efficiencies.

It is seen from the last two columns in Table II that there is a significant signal for the anomalous eμ(N_γ=0) and eh($N_\gamma \geq 0$) events. I will now assume that these anomalous two-prong events come from the production and decay of a heavy lepton according to the processes shown in reaction (1) in Section I, and I will show that our data are consistent with this assumption.[21]

B. eμ (N_γ = 0) events. Assuming the eμ events arise from the process:

$$e^+e^- \to \tau^+ + \tau^-$$
$$\tau^+ \to e^+\nu_e\bar{\nu}_\tau \qquad \tau^- \to \mu^-\bar{\nu}_\mu\nu_\tau$$

the number of corrected eμ events with $N_\gamma = 0$ is given by:

$$N_{e\mu} = \int Ldt\ \sigma(e^+e^- \to \tau^+\tau^-)\ 2\ B_e\ B_\mu\ A_{e\mu}$$

where: $\int Ldt$ = integrated luminosity

$$\sigma(e^+e^- \to \tau^+\tau^-) = \frac{21.71}{E^2_{beam}}\ \frac{\beta}{2}\ (3-\beta^2)\ \text{nb, where } \beta = \frac{v_\tau}{c}$$

$B_e(B_\mu)$ is the branching ratio for $\tau \to e\ \nu_e\ \nu_\tau(\mu\ \nu_\mu\ \nu_\tau)$

$A_{e\mu}$ is the acceptance of the apparatus for eμ events.[21]

Assuming $B_e = B_\mu$, we can calculate B_e from our data. The results are given in Table III for the three energy regions.

Table III. Measured branching ratios[22] $B_e(\tau \to e\ \nu_e\ \nu_\tau)$ and $B_h(\tau \to$ single charged hadron + neutrals). The branching ratios have been calculated assuming $B_e = B_\mu$, V-A coupling, a point production cross section for the τ, m(τ)=1.9 GeV, and $m(\nu_\tau) = 0.0$. Only statistical errors are shown.

$E_{c.m.}$ range (GeV)	$B_e(\tau \to e\ \nu_e\ \nu_\tau)$ (%)	$B_h(\tau \to$ single charged hadrons + neutrals), (%)
4.1 - 4.2	20.5 ± 8.2	36 ± 41
4.4 - 5.7	19.6 ± 5.2	48 ± 28
6.4 - 7.4	23.2 ± 4.4	43 ± 25
All three ranges combined	21.6 ± 3.1	43 ± 16

The three values of B_e are in good agreement, showing that the energy dependence of eμ production is consistent with the heavy lepton hypothesis. Combining the data and including an estimated 20% systematic error, we obtain:[22]

$$\boxed{B_e(\tau \to e\ \nu_e\ \nu_\tau) = (21.6 \pm 5.3)\%}$$

This is in good agreement with previous measurements[4,8-11] and with the theoretical expectation of 20%.[23]

C. eh ($N_\gamma \geq 0$) events

Assuming the eh events arise from the process:

$$e^+ e^- \to \tau^+ + \tau^-$$
$$\tau^+ \to e^+ \nu_e \bar{\nu}_\tau, \quad \tau^- \to \nu_\tau + \text{single charged hadron} + \text{possible additional neutrals}$$

the number of corrected events is given by:

$$N_{eh} = \int Ldt\, \sigma(e^+e^- \to \tau^+\tau^-)\, 2\, B_e\, B_h\, A_{eh}$$

where: N_{eh} is the sum of the eh events for $N_\gamma = 0$ and $N_\gamma > 0$

$\int Ldt$, σ are the same as before

B_h is the branching ratio for the decay $\tau \to$ single charged hadron + neutrals

A_{eh} is the acceptance of the apparatus for eh events,[21] calculated assuming only $\tau \to \pi\, \nu_\tau$, $\rho\, \nu_\tau$ contribute to two-prong eh events. We expect these decays to contribute 73% of the decays $\tau \to$ single charged hadron + neutrals.[23]

Using $B_e = (21.6 \pm 5.3)\%$, which is the result from the previous section, we can calculate B_h from our data. The results are given in Table III. Again, the three values of B_h are in good agreement. Combining the data and including an estimated 20% systematic error, we obtain:[22]

$$\boxed{B_h(\tau \to \text{single charged hadron} + \text{neutrals}) = (43 \pm 18)\%}$$

This is in agreement with the theoretical expectation of 45%.[23]

D. Momentum and Coplanarity Distributions. Figures 5(a)-5(c) show the corrected momentum distributions for the hadrons, muons and electrons in all the anomalous two-prong events, in terms of the variable r, defined as

$$r = \frac{p - p_o}{p_{max} - p_o}$$

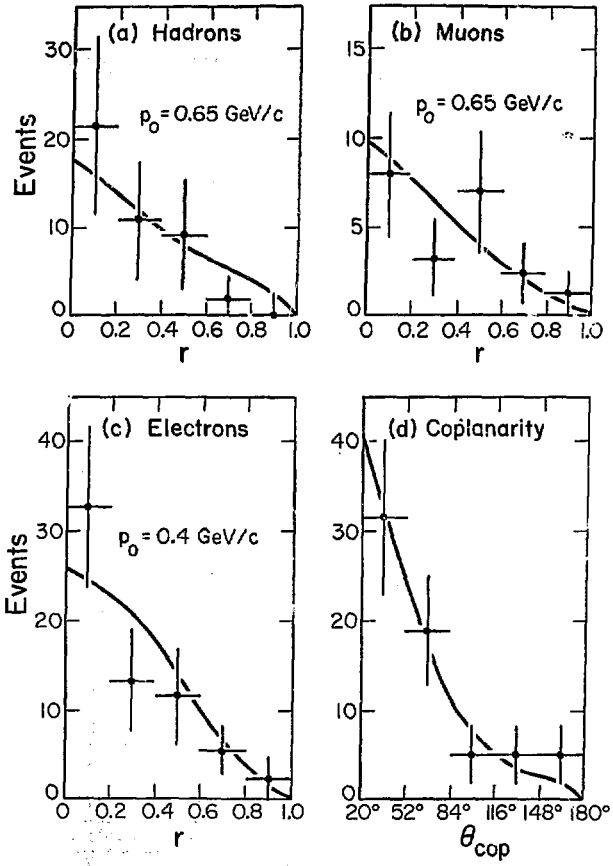

XBL 776-1241

Fig. 5 The distributions of the momentum variable $r \equiv (p-p_0)/(p_{max}-p_0)$ for a) the hadrons, b) the muons, and c) the electrons in the eμ and eh anomalous two-prong events. In (d) we have the coplanarity angle distribution for all the anomalous two-prong events. Data from all three energy regions have been combined. The curves show the expected distributions assuming heavy lepton production and decay.[21] They are normalized to the total number of events in each plot.

where: p = momentum of the particle

p_o = cut-off momentum (0.4 GeV/c for electrons; 0.65 GeV/c for muons and hadrons)

p_{max} = maximum momentum allowed in τ decay.[21]

Figure 5(d) shows the corrected coplanarity angle distribution for all the anomalous two-prong events.

The curves in Figure 5 show the expected momentum and coplanarity distributions assuming heavy lepton production and decay.[21] They are normalized to the total number of events in each plot. It is seen that the data are consistent with the heavy lepton hypothesis.

It should be stated again that in our measurement of the branching ratios we have assumed that a heavy lepton is the only source of the two-prong events, and have ignored a possible contribution from semi-leptonic decays of charmed particles. Thus, strickly speaking, the measured branching ratios should be considered as upper limits.

V. MULTIPRONG EVENTS[24]

A. Event Sample. We recall from Section I that the "multiprong" events are of the type:

$$e^+e^- \to e^\pm + (\geq 2 \text{ charged particles}) + n \cdot \gamma, \text{ with } n \geq 0$$

At least three charged particles are detected, and the electron is always identified in the lead-glass wall.

I will present here the results of the multiprong event analysis for data taken in four different center-of-mass energy ranges:[25]

$E_{c.m.}$ range (GeV)	Average $E_{c.m.}$ (GeV)	$\int Ldt$ (pb^{-1})
3.76-3.79	3.774	1.28
4.1 -4.2	4.16	1.01
4.4 -5.7	4.9	3.46
6.4 -7.4	7.0	5.37

Since the lowest $E_{c.m.}$ range is essentially at the top of the $\psi(3772)$ resonance, which decays into $D\bar{D}$,[26,27] the interpretation of the multiprong events there in terms of the semi-leptonic decay of the charmed D meson is quite straightforward. In the other $E_{c.m.}$ ranges, the interpretation is more complicated because a) we aren't sure of the exact production mechanism of D mesons (i.e. $e^+e^- \to DD^*$, D^*D^*, $D^*D^*\pi\pi$, ...), and b) there might be other charmed particles produced, such as F mesons or charmed baryons. The best we can do at this point in the analysis is to measure an average semi-leptonic branching ratio for "charmed particles" into electrons for each of the three highest center-of-mass energy ranges.

The multiprong events are selected using the following criteria:

1) The momentum of the particle in the lead-glass wall is > 300 MeV/c.

2) The particle in the lead-glass wall is identified as an electron using the criteria discussed in Section III.A. for multiprong events.

3) At least two other charged particles are detected in the Mark I detector or the lead-glass wall.

4) For the $E_{c.m.}$ range 3.76-3.79 GeV only, the momentum of each particle in the event (except the one identified as the electron) must be less than the maximum momentum kinematically allowed for D meson decay.

5) The event is rejected:

a) If any particle in the event has a momentum greater than half the beam energy, and is coplanar with any other particle in the event within 10°, or

b) If any two particles in the event each have a momentum greater than half the beam energy, and any particle in the event (other than the one in the lead-glass wall) is identified as an electron by the Mark I detector.

Both of the criteria in 5) above were designed to eliminate QED events like $e^+e^- \to e^+e^-\gamma$ or $e^+e^-\gamma\gamma$, with one or both photons converting to an e^+e^- pair.

These events are commonly called "multiprong Bhabha events."

For each center-of-mass energy range, the number of multiprong events which satisfy all of the above criteria are listed in the first line of Table IV under the heading of electron candidates.

Table IV. Multiprong events. See text for event selection criteria and discussion of backgrounds. $\sigma_e(p_e > 300$ MeV/c) is the cross section for multiprong events with an anomalous electron of momentum > 300 MeV/c, after the heavy lepton contribution is subtracted. These results are preliminary.

	Center-of-mass energy range (GeV)			
	3.76-3.79	4.1-4.2	4.4-5.7	6.4-7.4
Electron candidate events	55	54	139	146
Background events	23 ± 2	19 ± 2	52 ± 5	58 ± 6
Corrected events	46 ± 12	50 ± 12	119 ± 20	113 ± 19
Expected events from *heavy lepton* τ	0	6 ± 2	21 ± 6	18 ± 5
$\sigma_e(p_e > 300$ MeV/c) in nb	1.13±0.34	1.31±0.39	0.82±0.20	0.47±0.11

The expected number of background events from the backgrounds discussed in Section III. C. (i.e. from hadron misidentification, pion and kaon decay, and asymmetric photon conversions or Dalitz decays) are listed in the *second* line of Table IV. It is seen that ~ 40% of the electron candidates are due to background.

After subtracting the background events from the electron candidates, and correcting for the electron detection efficiency ($\bar{\varepsilon}$ ~ 75%) discussed in Section III. B., one has the number of corrected events shown in the third line of Table IV.

The production and decay of heavy leptons (τ) will contribute a small number of events to the multiprong events, as we have seen in Section I that the branching ratio for $\tau \rightarrow$ ($\geq$ 2 charged particles) + neutrals is ~15%.[23] Using this branching ratio, we have calculated[21] the expected contribution of the τ to the corrected events, and this is listed in line 4 in Table IV. It is seen that the τ contribution is typically ~15%.

Subtracting the τ contribution from the number of corrected events, and then correcting this result for a) the solid angle of the lead-glass wall (0.055 sr), b) for the detection efficiency of the other particles besides the electron (typically ~75-85%), and c) for several efficiencies for the data cuts whose product is ~80%, we can use the integrated luminosities given at the beginning of this Section to calculate the cross sections for multiprong events with an electron of momentum greater than 300 MeV/c. These are listed in the last line of Table IV. It is seen that we observe a substantial anomalous electron signal in all four energy ranges.

The momentum distributions for the electrons in the multiprong events are presented in Figure 6. The data in Figure 6 have been corrected for backgrounds and efficiencies, but the ~15% contamination due to the heavy lepton (τ) contribution at the higher center-of-mass energies has not been subtracted. It is seen that the electron spectrum hardens with increasing center-of-mass energy, and that there are indications that the peak momentum might be shifting slightly higher at the same time.

B. <u>B(D→eX) at the ψ(3772)</u>. The lowest center-of-mass energy range in this analysis, 3.76-3.79 GeV, corresponds to the ψ(3772) resonance.[15] The ψ(3772) appears to decay almost entirely into $D\bar{D}$,[26,27] which strongly suggests that the multiprong events at the ψ(3772) come from the decay of charmed D mesons

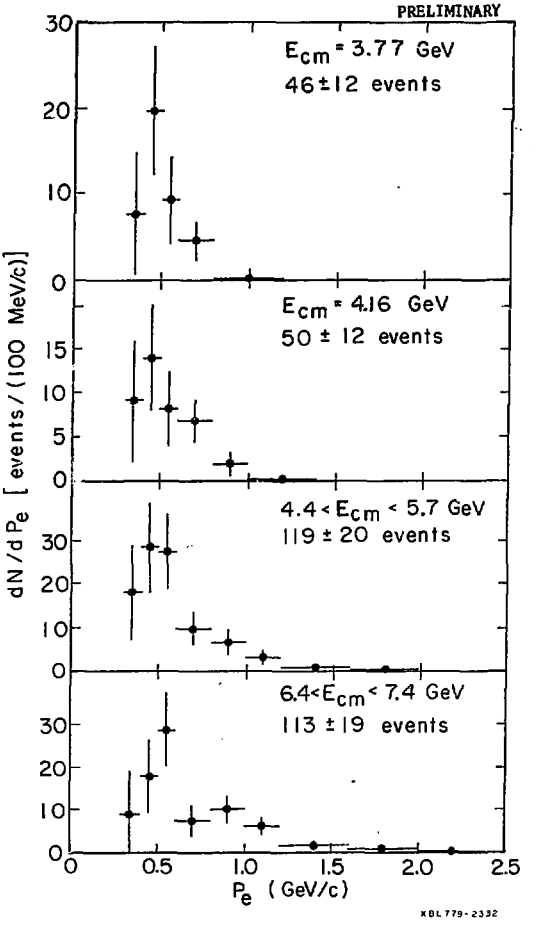

Fig. 6 The corrected momentum distributions above 300 MeV/c for the electrons in the multiprong events, for the four center-of-mass energy regions. The data are corrected for backgrounds and efficiences, but not for the ~15% heavy lepton contribution in the three highest energy regions.

via reaction (2) in Section I (with n = 0). In Figure 7 we show again our corrected momentum distribution for the electrons in the multiprong events at the $\psi(3772)$, along with the momentum spectra expected from D meson production in $e^+e^- \to \psi(3772) \to D\bar{D}$ with subsequent semi-leptonic decay into $\pi e\nu_e$, $Ke\nu_e$ or $K^*e\nu_e$ (for both V + A and V - A forms for the current which couples D to K^*).[28] The data are consistent with the Cabibbo-favored decay modes $D \to Ke\nu_e$ (confidence level = 49%), $D \to K^*e\nu_e$ (V-A) (CL=54%) or $D \to K^*e\nu_e$ (V+A) (CL=79%), but are inconsistent with coming entirely from the Cabibbo-suppressed mode $D \to \pi e\nu_e$ (CL=2%). The data are also inconsistent with the purely leptonic decay $D \to e\nu_e$ which would produce a flat electron spectrum from about 810 MeV/c to 1080 MeV/c. If we combine the $Ke\nu_e$ and $K^*e\nu_e$ (V-A) spectra for a fit to the data, we find the $Ke\nu_e$ fraction to be (45±35)%.

Assuming that the multiprong signal at the $\psi(3772)$ comes entirely from D meson production and decay,[29] and that the $\psi(3772)$ decays entirely into $D\bar{D}$, we can calculate the semileptonic branching ratio for D meson decay into an electron plus other particles:

$$B(D \to eX) = \frac{\sigma_e(p_e > 300\ \text{MeV/c})/A(p\ \text{cut})}{\sigma(D)}$$

where

$\sigma_e(p_e > 300\ \text{MeV/c}) = 1.13 \pm 0.34$ nb from Table IV

A(p cut) is the correction for the part of the electron spectrum which falls below our cutoff value of 300 MeV/c. As a model, we take the average of the decay spectrum for $D \to Ke\nu_e$ and $K^*e\nu_e$ (V-A) as shown in Figure 7. We obtain A(p cut) = 0.82

$\sigma(D)$ is the cross section for D production, which we have previously determined to be 20.6 ± 4.3 nb.[26]

We thus find:[30] $\boxed{B(D \to eX) = (6.7 \pm 2.4)\%}$

C. B(charmed particles → eX) at several $E_{c.m.}$ As we discussed, it is only possible to give an average semi-leptonic branching ratio for "charmed

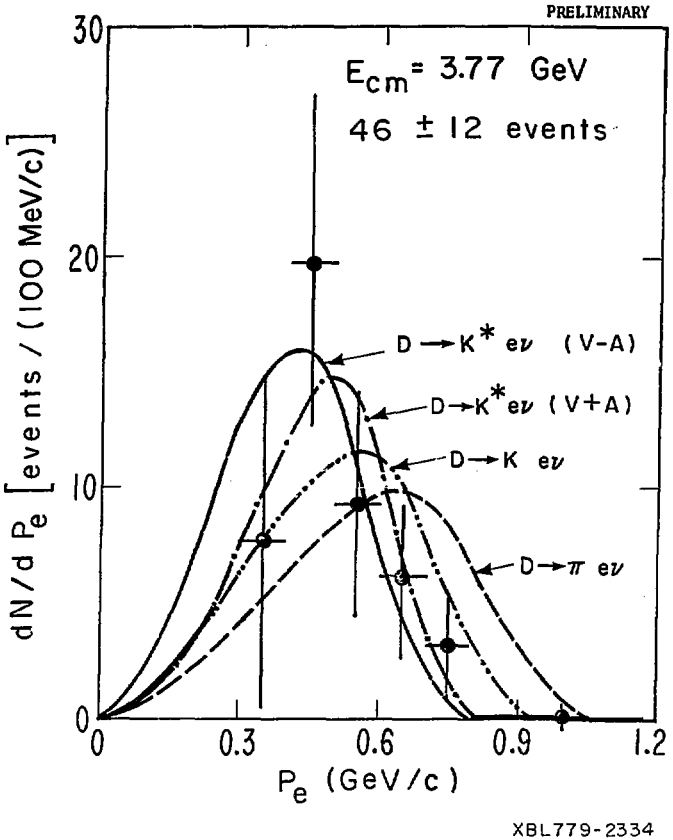

Fig. 7 The corrected momentum distribution above 300 MeV/c for the electrons in the multiprong events at the ψ(3772). The curves show the electron momentum spectra expected from D meson production (via $e^+e^- \to D\bar{D}$) and decay (via $D \to \pi e \nu_e$, $K e \nu_e$ and $K^* e \nu_e$), based on the calculations of Ali and Yang.[28] The curves are normalized above 300 MeV/c to the total number of events.

particles" into electrons for each of the three highest center-of-mass energy ranges, because we can't separate D decays from other charmed particle decays in our data. We write:

$$B(c \to eX) = R_e/2\, R_{charm}$$

where: $c \equiv$ "charmed particles"

$$R_e = \frac{\sigma_e(p_e > 300\ \text{MeV/c})/A(p\ \text{cut})}{\sigma(e^+e^- \to \mu^+\mu^-)}$$

$$R_{charm} = \frac{\text{cross section for production of a pair of charmed particles}}{\sigma(e^+e^- \to \mu^+\mu^-)}$$

To evaluate R_e we again need A(p cut), which is the correction for the part of the electron spectrum which falls below our cutoff value of 300 MeV/c. To determine A(p cut) we need to know the momentum spectrum of the electron in the "charmed particle" decays, and we need to know how the "charmed particles" are produced so that we can properly Lorentz boost the spectra. As an approximation we have chosen a reasonable production process for D meson production for each of the four center-of-mass energy ranges, and assumed the D's decay to $Ke\nu_e$ or $K^*e\nu_e$(V-A). The assumed production processes are:[31]

$E_{c.m.}$ (GeV)	Production Process
3.772	$D\bar{D}$
4.16	D^*D^*
4.4-5.7	D^*D^*
6.4-7.4	$D^*D^*\pi\pi$

The resulting spectra are shown in Figures 8-10, along with our data.[28] The agreement is satisfactory, and we average the $Ke\nu_e$ and $K^*e\nu_e$(V-A) spectra to obtain A(p cut), and thus R_e. The result is the first column in Table V.

PRELIMINARY

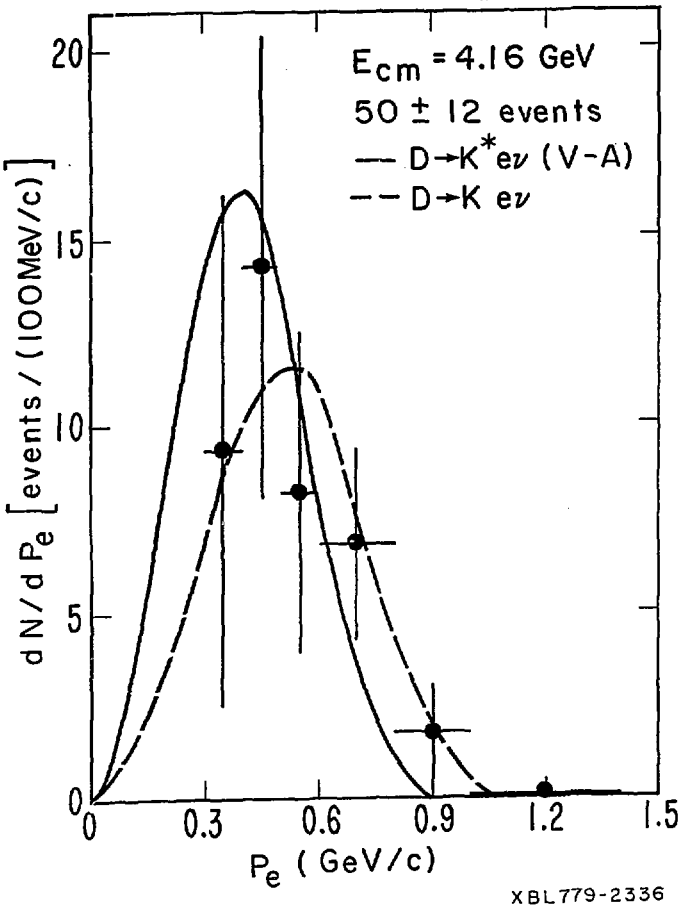

Fig. 8 The corrected momentum distribution above 300 MeV/c for the electrons in the multiprong events at $E_{c.m.}$ = 4.16 GeV. The ~15% heavy lepton contribution has not been subtracted. The curves show the electron momentum spectra expected from D meson production (via $e^+e^-\to D^*D^*$) and decay (via $D\to Ke\nu_e$ and $K^*e\nu_e$ (V-A)), based on the calculations of Ali and Yang.[28] The curves are normalized above 300 MeV/c to the total number of events.

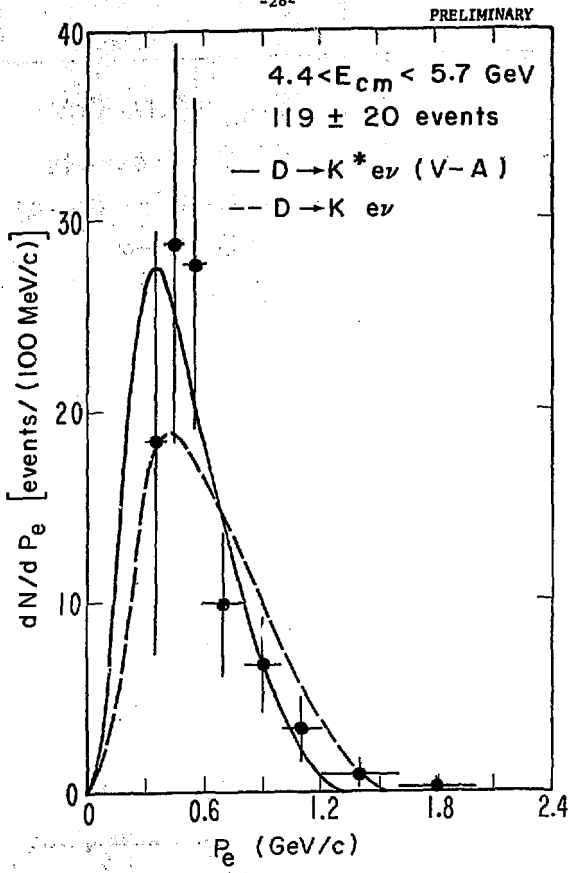

XBL779-2333

Fig. 9 The corrected momentum distribution above 300 MeV/c for the electrons in the multiprong events in the $E_{c.m.}$ region 4.4-5.7 GeV. The ~15% heavy lepton contribution has not been subtracted. The curves show the electron momentum spectra expected from D meson production (via $e^+e^- \to D^*D^*$) and decay (via $D \to Ke\nu_e$ and $K^*e\nu_e$(V-A)), based on the calculations of Ali and Yang.[28] The curves are normalized above 300 MeV/c to the total number of events.

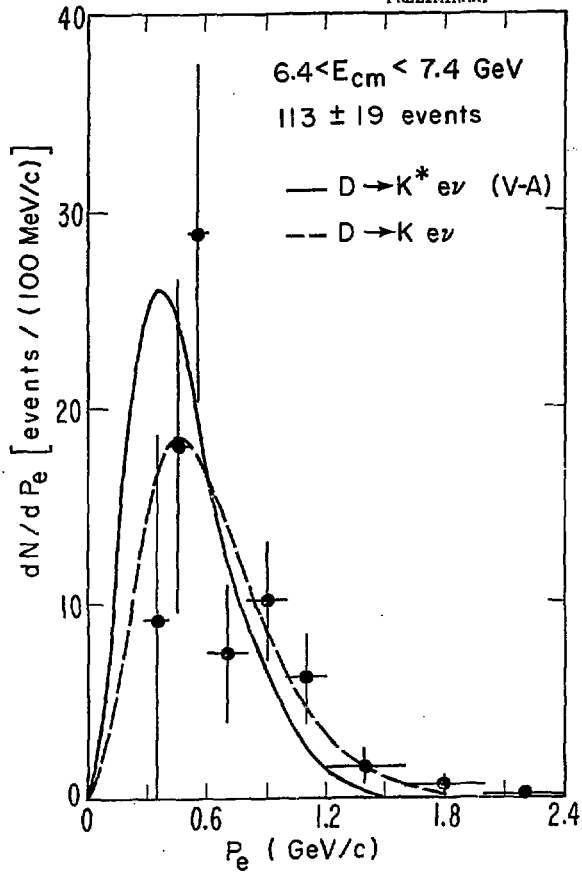

XBL779-2335

Fig. 10 The corrected momentum distribution above 300 MeV/c for the electrons in the multiprong events in the $E_{c.m.}$ region 6.4-7.4 GeV. The ~15% heavy lepton contribution has not been subtracted. The curves show the electron momentum spectra expected from D mason production (via $e^+e^- \to D^*D^*\pi\pi$) and decay (via $D \to Ke\nu$ and $K^*e\nu_e$(V-A)), based on the calculations of Ali and Yang.[28] The curves are normalized above 300 MeV/c to the total number of events.

Table V. Multiprong events. For definitions of the quantities, see the text. The results are preliminary.

$E_{c.m.}$ range (GeV)	R_e	R_{charm}	$B(c \to eX)$ (%)
3.76-3.79 [ψ(3772)]	0.23±0.07	1.7±0.3	6.7±2.4
4.1-4.2	0.32±0.10	2.1±0.5	7.7±3.0
4.4-5.7	0.28±0.07	1.9±0.5	7.4±2.8
6.4-7.4	0.33±0.08	1.9±0.4	8.7±3.2

To evaluate R_{charm} we assume:

$$R_{charm} = R - R_\tau - R_{old}$$

where:

$$R = \sigma(e^+e^- \to \text{hadrons})/\sigma_{\mu\mu}$$

R_τ is the contribution to R from $e^+e^- \to \tau^+\tau^-$, and equals $\frac{\beta}{2}(3-\beta^2)$ with $\beta = v_\tau/c$.

We assume $m_\tau = 1.9$ GeV.

R_{old} is the constant value of R below the charm threshold. We take $R_{old} = 2.6$.

The values of R_{charm} so determined are listed in the second column in Table V.[32]

Having R_e and R_{charm}, we thus can calculate $B(c \to eX)$, which is listed in the last column in Table V. Figure 11 shows $B(c \to eX)$ as a function of the center-of-mass energy. There does not seem to be any large variation of the branching ratio with energy.

The values of $B(c \to eX)$ obtained here agree within errors with those obtained at DORIS,[13,33] but seem to be systematically lower. This is probably due to the long standing fact that the measurements of the total hadronic cross

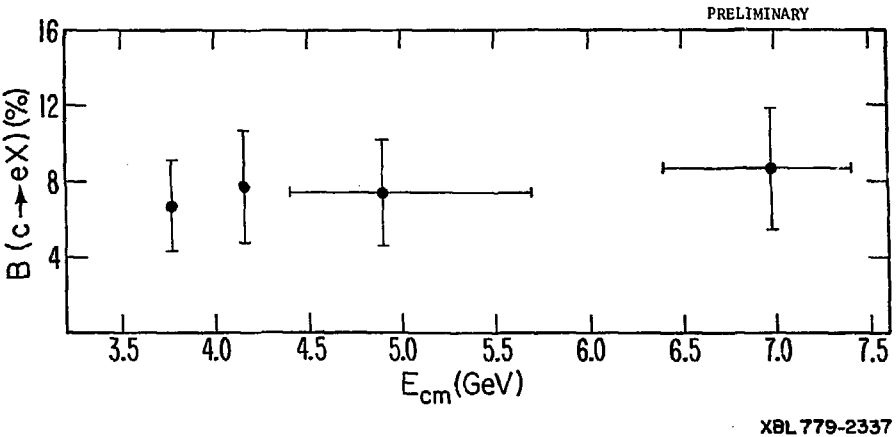

Fig. 11 The semi-leptonic branching ratio of charmed particles into electrons as a function of the center-of-mass energy.

section (and thus R) at SPEAR with the Mark I detector have always been higher then those measured at DORIS.[34]

VI. SUMMARY.

1) We observe anomalous electron production in two-prong events which is consistent with the heavy lepton hypothesis. Assuming all these events arise from the production and decay of a heavy lepton, τ, we have measured the branching ratios:[22]

$$B_e(\tau \to e\nu_e\nu_\tau) = (21.6 \pm 5.3)\%$$

$$B_h(\tau \to \text{single charged hadron + neutrals}) = (43 \pm 18)\%$$

2) We observe anomalous electron production in multiprong events. At the $\psi(3772)$ the electron momentum spectrum is consistent with the Cabibbo-favored semi-leptonic decays of the charmed D meson, and using efficiencies averaged over $D \to Ke\nu_e$ and $K^*e\nu_e(V\text{-}A)$, we have measured the semi-leptonic branching ratio of the D into electrons:[30]

$$B(D \to eX) = (6.7 \pm 2.4)\%$$

For higher center-of-mass energies we have obtained average semi-leptonic branching ratios for charmed particles into electrons under similar assumptions. Our preliminary results are:

$E_{c.m.}$ (GeV)	$B(c \to eX)$ (%)
4.1-4.2	7.7 ± 3.0
4.4-5.7	7.4 ± 2.8
6.4-7.4	8.7 ± 3.2

I sincerely acknowledge the large contribution that has been made by the members of the Lead-Glass Wall collaboration[1] in obtaining the results presented here. I also thank Mrs. Josephine Barrera for her help in typing this paper.

REFERENCES AND FOOTNOTES

1. The members of the Lead-Glass Wall collaboration are: A. Barbaro-Galtieri, R. Ely, J. M. Feller, A. Fong, P. Lecomte, R. J. Madaras, T. S. Mast, M. T. Ronan, R. R. Ross, B. Sadoulet, T. G. Trippe, V. Vuillemin, (Lawrence Berkeley Laboratory and Department of Physics, University of California at Berkeley); J. M. Dorfan, G. J. Feldman, G. Hanson, J. A. Jaros, B. P. Kwan, A. M. Litke, D. Lüke, J. F. Martin, M. L. Perl, I. Peruzzi, M. Piccolo, T. P. Pun, P. A. Rapidis, D. L. Scharre (Stanford Linear Accelerator Center and Department of Physics, Stanford University); B. Gobbi, D. H. Miller (Department of Physics and Astronomy, Northwestern University); S. I. Parker, D. E. Yount (Department of Physics and Astronomy, University of Hawaii).

2. Results from the same experiment on non-leptonic decays of D mesons are presented by G. J. Feldman in these Proceedings.

3. J.-E. Augustin et al., Phys. Rev. Lett. 34, 233 (1975); G. J. Feldman and M. L. Perl, Phys. Reports 19C, 233 (1975), Appendix A; F. Vannucci et al., Phys. Rev. D15, 1814 (1977).

4. M. L. Perl et al., Phys. Rev. Lett. 35, 1489 (1975)

5. M. L. Perl et al., Phys. Letters 63B, 466 (1976).

6. A. Barbaro-Galtieri et al., Lawrence Berkeley Laboratory report number LBL-6458 (1977) and Stanford Linear Accelerator Center report number SLAC-PUB-1976 (1977), to be published in Phys. Rev. Lett.

7. M. Cavalli-Sforza et al., Phys. Rev. Lett. 36, 558 (1976); see also an interpretation of these data by G. Snow, Phys. Rev. Lett. 36, 766 (1976).

8. G. J. Feldman et al, Phys. Rev. Lett. 38, 117 (1977)

9. M. L. Perl et al., Stanford Linear Accelerator Center report number SLAC-PUB-1997 (1977) and Lawrence Berkeley Laboratory report number LBL-6731 (1977), submitted to Phys. Letters.

10. J. Burmester et al., Phys. Letters 68B, 297 (1977).

11. J. Burmester et al., Phys. Letters 68B, 301 (1977).

12. R. Brandelik et al., DESY report DESY 77/36 (1977).

13. Recent DESY results on anomalous electron production in electron-positron annihilations are presented by W. de Boer in these Proceedings.

14. The predictions are based on Y. S. Tsai, Phys. Rev. D4, 2821 (1971), and H. B. Thacker and J. J. Sakurai, Phys. Letters 36B, 103 (1971), as discussed by G. J. Feldman in Proceedings of the 1976 Summer Institute on Particle Physics (SLAC, 1976), also issued as SLAC report number SLAC-PUB-1852 (1976).

15. P. A. Rapidis et al., Phys. Rev. Lett. 39, 526 (1977).

16. R. F. Althaus et al., IEEE Trans. Nucl. Sci. NS-24, 218 (1977) and NS-24, 408 (1977)

17. More details on the lead-glass detector can be found in J. Feller et al., Lawrence Berkeley Laboratory report number LBL-6466 (1977).

18. R. J. Madaras et al., Lawrence Berkeley Laboratory report number LBL-6767 (1977), in preparation.

19. Two of the anomalous two-prong events have both the electron and the other particle identified in the lead-glass wall.

20. After we published our two-prong event results (see Reference 6), we found that the $\int Ldt$ that we had used was too small by about 8%. The integrated luminosities listed here are the correct ones for the two-prong event analysis.

21. We take the properties of the heavy lepton, τ, to be: $m(\tau) = 1.9$ GeV, $m(\nu_\tau) = 0.0$, V-A weak interaction coupling.

22. Because of the 8% correction in $\int Ldt$ (see Reference 20), these branching ratios are 4% smaller than the ones published in Reference 6.

23 See Table I in Section I.

24. The results of the multiprong event analysis in this written version of my talk are different (by less than one-half the quoted errors) from the results I originally presented. This is because a) the analysis now includes a larger data sample, and b) the analysis has been improved since the talk.

25. The integrated luminosities here are different than for the two-prong event analysis, because of slightly different data samples.

26. I. Peruzzi et al., Stanford Linear Accelerator Center report number SLAC-PUB-2012 and Lawrence Berkeley Laboratory report number LBL-6755 (1977).

27. See G. J. Feldman's talk in these Proceedings.

28. The electron momentum spectra (for D's at rest) are taken from the calculations of A. Ali and T. C. Yang, Phys. Letters 65B, 275 (1976) and A. Ali, private communication. We then Lorentz boost them with a Monte Carlo program to take into account the D momentum.

29. If the $\psi(3772)$ is above the threshold for $\tau^+\tau^-$ production, an anomalous electron signal may also arise from decays of the heavy lepton τ. From preliminary measurements on $e\mu$ events at the $\psi(3772)$ (see M. L. Perl, Proceedings of the 1977 International Symposium on Lepton and Photon Interactions at High Energies, Hamburg, 1977, to be published) we estimate that 6% of the anomalous electron events can come from this source. Taking account of $\tau^+\tau^-$ production would also lead to a decrease in the value of $\sigma(D)$ by about 12%; the net effect is to raise our value for the branching ratio of D to electrons from 6.7% to 7.1%. For additional information on $e\mu$

and eh two-prong events at $E_{c.m.} = 3.77$ GeV (with the electron in the LGW), see the talk of A. Barbaro-Galtieri, Proceedings of the 1977 International Symposium on Lepton and Photon Interactions at High Energies, Hamburg, 1977, to be published.

30. This is a preliminary value. The final value is (7.2 ± 2.8)%, which was obtained after this paper was written. See J. Feller et al., Lawrence Berkeley Laboratory report number LBL-6772 (1977).

31. The production process for the center-of-mass energy 3.772 GeV is listed here only for completeness. We saw in Section V.B. that the $\psi(3772)$ decays almost entirely into $D\bar{D}$ (see References 26 and 27).

32. The results for the $\psi(3772)$ were discussed in Section V.B., and are listed here only for completeness. R_{charm} for the $\psi(3772)$ is obtained by dividing the experimentally measured cross section for D production, $\sigma(D)$, by $2\sigma_{\mu\mu}$. See reference 26 for $\sigma(D)$.

33. W. Braunschweig et al., Phys. Letters 63B, 471 (1976); J. Burmester et al., Phys. Letters 64B, 369 (1976); R. Brandelik et al., DESY preprint DESY 77/41 (1977).

34. See the talks of V. Luth and W. de Boer in these Proceedings.